

## Resolving eddies by local mesh refinement

S. Danilov<sup>a,b,\*</sup>, Q. Wang<sup>a</sup>

<sup>a</sup> Alfred Wegener Institute, Helmholtz Centre for Polar and Marine Research, Bremerhaven 27515, Germany

<sup>b</sup> A. M. Obukhov Institute of Atmospheric Physics RAS, Moscow, Russia



### ARTICLE INFO

#### Article history:

Received 5 May 2015

Revised 12 July 2015

Accepted 17 July 2015

Available online 26 July 2015

#### Keywords:

Unstructured meshes

Nesting

Hollingsworth instability

### ABSTRACT

Nesting in large-scale ocean modeling is used for local refinement to resolve eddy dynamics that would not be accessible otherwise. Unstructured meshes offer this functionality too by adjusting their resolution according to some goal function. However, by locally refining the mesh one does not necessarily achieve the goal resolution, because the eddy dynamics, in particular the ability of eddies to release the available potential energy, also depend on the dynamics on the upstream coarse mesh. It is shown through a suite of experiments with a zonally re-entrant channel that baroclinic turbulence can be out from equilibrium in wide (compared to a typical eddy size) zones downstream into the refined area. This effect depends on whether or not the coarse part is eddy resolving, being much stronger if it is not. Biharmonic viscosity scaled with the cube of grid spacing is generally sufficient to control the smoothness of solutions on the variable mesh. However, noise in the vertical velocity field may be present at locations where the mesh is varied if momentum advection is implemented in the vector invariant form. Smoothness of vertical velocity is recovered if the flux form of momentum advection is used, suggesting that the noise originates from a variant of the Hollingsworth instability.

© 2015 Elsevier Ltd. All rights reserved.

### 1. Introduction

Nesting is a widely used tool in studies of large-scale ocean circulation, helping to resolve eddy dynamics over a limited area. The interest to nesting is motivated by several factors. For one thing, running a global fine-resolution model can still be prohibitively expensive if one's focus is on the regional dynamics. For another, the Rossby radius of deformation is rather small at high latitudes, so that resolving eddies there may require excessively fine resolution elsewhere if the resolution is uniform. There are numerous examples in the literature showing the success of the nesting approach (see, e.g., Chanut et al. (2008), Durgadoo et al. (2013), Mertens et al. (2014)), while the general principles of two-way nesting algorithms are reviewed by Debreu and Blayo (2008).

Unstructured meshes offer geometric flexibility and freedom with respect to mesh design, and may serve as an alternative to the nesting approach for structured meshes. In addition to applications where the unstructured meshes are used to better represent the domain geometry (see, e.g., Timmermann and Hellmer (2013), Wekerle et al. (2013)), the use of mesh refinement as a tool to resolve eddies is already a proven concept (see Ringler et al., 2013). However, if the mesh resolution is allowed to vary, questions arise about the optimal

way and consequences of varying it. Physical principles governing the selection of mesh resolution depend on applications, and not surprisingly, there is no unique solution. The review by Greenberg et al. (2007) mentions some aspects, and each real application may add new details.

We focus below only on one aspect of the problem related to the use of locally refined meshes to resolve eddy regimes. The amplitude of eddy motions simulated by a numerical model in a particular subdomain depends not only on the local resolution, but also on the presence of upstream perturbations, which serve as the seeds from which perturbations grow, and facilitate the release of available potential energy. While this remark may seem trivial, its implications can be very easily underestimated, and this study seeks to address them in a qualitative way. Although we deal with unstructured meshes, the results reported below can be of interest to a wider community of ocean modelers working with nesting tools on standard structured meshes.

We consider a baroclinically unstable eastward flow in a zonally-reentrant channel, where the baroclinicity is maintained through forcing at its southern (warming) and northern (cooling) walls. A linear equation of state is used with the temperature being the only scalar field influencing the density. The flow is simulated on triangular meshes composed of nearly equilateral triangles. The resolution varies in the zonal direction, and by observing the flow variability along the channel the effect of the change in the mesh resolution is assessed.

\* Corresponding author. Tel.: +49 471 48311764.

E-mail address: [Sergey.Danilov@awi.de](mailto:Sergey.Danilov@awi.de) (S. Danilov).

A remark is due from the very beginning. Although the mesh refinement is discussed, the dissipative operators are always varied accordingly, and the refinement means not only smaller scales but simultaneously smaller coefficients in explicit dissipative operators, and similar reduction in effective implicit dissipation associated with upwinding or flux limiting in transport equations. These two aspects (refinement and reduced dissipation coefficients) are inseparable, for dissipative operators are always designed to dispose of eddy variance of scalars and the eddy enstrophy on the grid scale. According to linear instability theory the wavelength of the most unstable wave (we take the Eady instability problem as an example) scales as  $\lambda \approx 3.9\pi L_R$  where  $L_R = NH/\pi f$  is the first internal Rossby radius,  $N$  is the buoyancy frequency,  $f$  is the Coriolis parameter and  $H$  is the fluid thickness. On meshes called eddy-permitting ( $1/3$ – $1/4^\circ$  at midlatitudes), eddies with the size of  $\lambda/2$  can already be well represented, and yet it is well known that this resolution is by far insufficient. The point is that the accompanying subgrid dissipation still turns out to be too high so that only a part of the extracted available potential energy (APE) is fluxed back to maintain kinetic energy at large scales, while the other part is lost to subgrid dissipation on small scales (see Jansen and Held (2014) for the spectral analysis of the APE release rate and energy transfers on eddy-permitting and resolving meshes). According to the results obtained in Jansen and Held (2014) in simulations with a biharmonic Leith subgrid operator, the APE release rate saturates at resolutions between 2 and 3 grid intervals per  $L_R$ , which as we shall see, also agrees with this study. Note also that this correlates with the analysis of Hallberg (2013) for a related topic.

Our main goal below is to explore the response of turbulent flow to changes in mesh resolution, concentrating on the retardation and overshoots in eddy variability, and also on the ability to maintain smooth solutions in domains where resolution varies. Since mesh refinement also implies reduced dissipation and higher variability, a question on whether the dissipative operators can control the smoothness of solutions in regions where the resolution is adjusted back from fine to coarse one is tightly linked to the main goal.

## 2. Configuration and model

Most of the experiments are carried out in a zonally-reentrant channel  $L = 40^\circ$  long ( $0^\circ\text{E}$ – $40^\circ\text{E}$ ) occupying the latitude belt between  $30^\circ\text{N}$  and  $45^\circ\text{N}$ . The geometry is spherical. There are 24 unevenly distributed layers going down to 1600 m. Triangular surface meshes of variable resolution are used. The basic coarse resolution is  $1/3^\circ$ , and the basic fine resolution is  $1/12^\circ$ , giving the mesh refinement (or stretching) factor, measured as the ratio of the largest to the smallest mesh edges,  $r = 4$ . Meshes are refined via relatively narrow transitional zones centered in most cases at  $\phi_w = 7.5^\circ\text{E}$  and  $\phi_e = 32.5^\circ\text{E}$ , so that more than a half of the domain is well resolved, and the other part is left coarse. The mesh resolution (edge length)  $h$  varies according to the hyperbolic tangent,

$$h = h_0(r + 0.5(r - 1)(-\tanh((\phi - \phi_w)/w_t) + \tanh((\phi - \phi_e)/w_t))) \quad (1)$$

where  $h_0$  is the side of the smallest triangle, and  $w_t$  (in degrees) defines the width of the transitional zone. There are some variations of this basic setup. The parameters of the meshes used in different runs are presented in Table 1.

The density depends linearly on the temperature,  $\rho - \rho_r = -\rho_r\alpha(T - T_r)$ , with  $\rho_r$  and  $T_r$  the constant reference values and  $\alpha = 2.5 \times 10^{-4} \text{K}^{-1}$  the thermal expansion coefficient. The initial temperature distribution is linear in the meridional direction with the gradient  $T_{0y} = -0.5 \times 10^{-5} \text{K/m}$  and also in the vertical direction with the gradient  $T_{0z} = 8 \times 10^{-3} \text{K/m}$  in the entire channel. There are buffer zones  $1.5^\circ$  wide adjacent to the northern and southern walls where the temperature is relaxed to the initial one over the entire depth. The inverse relaxation time scale varies linearly from  $(3 \text{ day})^{-1}$  at the

**Table 1**

Geometrical parameters of meshes used, see Eq. (1).  $\phi_e$  is always symmetric to  $\phi_w$  with respect to the center of the mesh. The second and third columns specify the coarse and fine resolution. All quantities are in degrees.

Run	$rh_0$	$h_0$	$w_t$	$\phi_w$	$L$
A	1/3	1/12	1	7.5	40
A'	1/3	1/12	2.5	7.5	40
B	1/3	1/18	1.5	7.5	40
C	1/3	1/12	1.5	7.5	60
C'	1/3	1/12	4.5	10	60
D	1/6	1/24	1.5	7.5	40
E	1/9	1/36	1.5	10	40

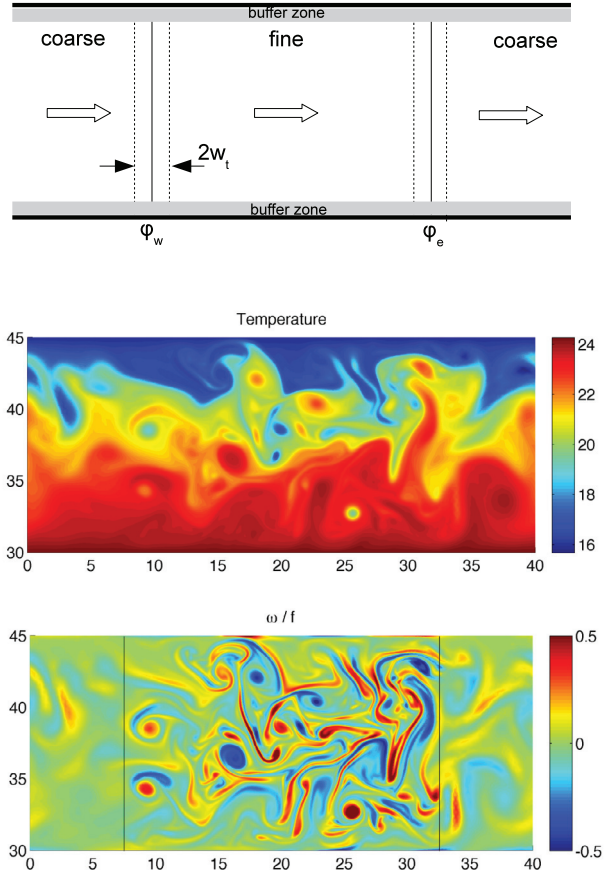


**Fig. 1.** Top: Setup schematics. Large arrows indicate the flow direction. The solid meridional lines show the centers of transitional zones, the dashed lines mark the transitional zones, as described by Eq. (1). Middle and bottom: Snapshots of temperature ( $^\circ\text{C}$ ) and relative vorticity (normalized by the local value of the Coriolis parameter) at approximately 100 m depth in case A. While only the sharpness of temperature filaments reveals the presence of mesh refinement in the middle panel, the relative vorticity field shows the formation of eddies on the fine mesh and their decay on the coarse mesh.

wall to zero outside the  $1.5^\circ$  zones. A small sinusoidal perturbation is applied to the temperature to speed up the development of the baroclinic instability, which equilibrates in about half a year. We only deal with short runs of several years (4 or 5) in duration and present the results averaged over the entire period of integration excluding the first year. While this is certainly insufficient to obtain stationary patterns of eddy variances, it is sufficient to draw qualitative conclusions for our questions. The configuration is schematically presented in the top panel of Fig. 1.

Download English Version:

<https://daneshyari.com/en/article/4551976>

Download Persian Version:

<https://daneshyari.com/article/4551976>

[Daneshyari.com](https://daneshyari.com)